ITALIAN NATIONAL AGENCY FOR NEW TECHNOLOGIES, ENERGY AND SUSTAINABLE ECONOMIC DEVELOPMENT

Progetti EU CAMS su assimilazione dati satellitari e sviluppo modelli di aerosol

M. MIRCEA[1], A. BOLIGNANO[1], M. ADANI[1], G. BRIGANTI[1], F. RUSSO[1], M. D'ISIDORO[1], A. PIERSANTI[1], A. D'AUSILIO[2], G. DE MOLINER[3], C. SILIBELLO[2]

[1] Italian National Agency for New Technologies, Energy and Sustainable Economic Development (ENEA), Via Martiri di Monte Sole 4, 40129 Bologna, Italy

[2] ARIANET srl, 20159 Milano, Via Benigno Crespi 52, Italy.

[3] Department of Civil and Environmental Engineering, Politecnico di Milano, Piazza Leonardo da Vinci 32, Milan, 20133, Italy

XII Giornata della Modellistica in ARIA(NET), 25 marzo 2025

CAMAERA(Copernicus Atmosphere Monitoring Service AERosol Advancement)
camaera-project.eu

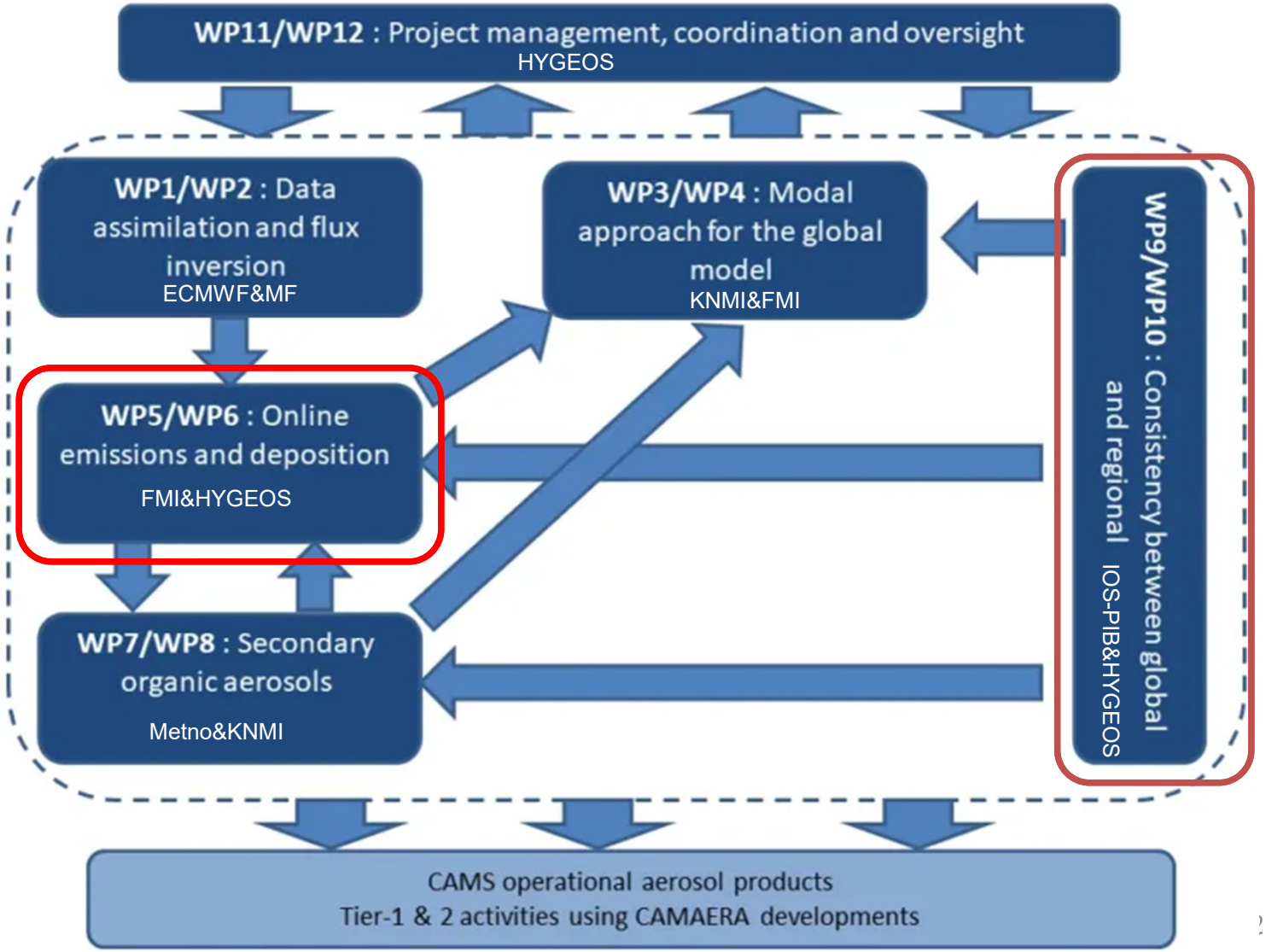

CAMAERA

WP5-6 Online emissions and deposition, implementation; Online emissions and deposition, test and evaluation

WP5 is led by Mikhail Sofiev (FMI) and Samuel Remy (HYGEOS, project coordinator)

Task 5.1 – Development of new desert dust and sea-salt aerosol emission schemes (lead FMI/HYGEOS contributors METNorway

- Machine learning approach for sea-salt aerosol emissions in the IFS with possible use in regional models
- Sea-salt aerosol emission schemes based on recent chamber experiments with possible use in regional models
- Implementation into the IFS and SILAM of a scheme that represents high latitude dust
- Development of a gridded version of the NORTRIP road dust emissions scheme and implementation into EMEP, EURAD-IM and LOTOS

Task 5.2 – Interactive ammonia emissions (lead FMI contributors FZJ)

- Implementation of FANv2 in SILAM, evaluation against regional inventories of ammonia emissions
- Collection of activity data as an input to FANv2

Task 5.3 – Dry deposition (lead TNO/HYGEOS, contributors FMI, SMHI, ENEA)

- 0D dry deposition intercomparison and evaluation with ground observations over different surfaces. Participant models are IFS, LOTOS-EUROS, GEM-AQ, SILAM, MATCH, MINNI.
- Extension of the dry deposition scheme of LOTOS-EUROS

WP6 is led by Mikhaïl Sofiev (FMI) and Samuel Remy (HYGEOS, project coordinator)

Task 6.1 – Development of new desert dust and sea-salt aerosol emission schemes (lead FMI/HYGEOS contributors MF)

- Machine learning approach for global desert dust aerosol emissions
- Implementation of the newly developed sea-salt and desert dust emission schemes into MOCAGE
- Improvement and evaluation of the Fire Forecasting System, implementation into SILAM and the IFS; evaluation on simulated AOD and PM particularly focusing on specific fire events

Task 6.2 – Interactive ammonia emissions (lead FMI contributors FZJ)

- Implementation of the crop specific management profiles
- Extension of the process model used to simulate emission reductions from tillage and other practices that incorporate the fertilizer to the soil matric
- Implementation of FANv2 in IFS and EURAD-IM, evaluation against regional inventories of ammonia emissions
- Evaluation of the impact of FANv2 ammonia emissions on global and regionally simulated PM2.5, ammonium aerosol at surface, ammonia burden against CrIS retrievals and on nitrogen deposition fluxes

Task 6.3 – Dry deposition (lead TNO/HYGEOS, contributors FMI, SMHI, ENEA)

- Implementation and test of the LOTOS-EUROS dry deposition scheme into the IFS
- Update of the 0D dry deposition intercomparison

Model description: Pleim and Ran (2011) – PR11

Table 1
Detailed mechanistic expressions used for particle dry deposition velocity and resistance parameters for monodisperse and sectional approaches.

Scheme	V_d	R_a	R_s
PR11[a]	$\frac{V_g}{1 - e^{-V_g(R_a+R_s)}}$	$\frac{\ln\left(\frac{Z_R}{Z_0}\right) - \Psi_H}{\varphi_{hn}\kappa u_\star}$	$\frac{1}{F_f u_\star E_{Tot}}$
OFF[b]	$\frac{V_g}{1 - e^{-V_g(R_a+R_s)}}$	$\frac{\ln\left(\frac{Z_R}{Z_0}\right) - \Psi_H}{\varphi_{hn}\kappa u_\star}$	$\frac{1}{F_f u_\star E_{Tot}}$
VGLAI[c]	$\frac{V_g}{1 - e^{-V_g(R_a+R_s)}}$	$\frac{\ln\left(\frac{Z_R}{Z_0}\right) - \Psi_H}{\varphi_{hn}\kappa u_\star}$	$\frac{1}{(1 + f_{veg}(\max(LAI - 1,\ 0)))F_f u_\star E_{Tot}}$
Z01[d]	$V_g + \frac{1}{R_a + R_s}$	$\frac{\ln\left(\frac{Z_R}{Z_0}\right) - \Psi_H}{\varphi_{hn}\kappa u_\star}$	$\frac{1}{\varepsilon_0 u_\star E_{Tot} R_1}$

V_g = settling velocity: $V_g = \frac{\rho d_p^2 g C}{18\mu}$ (m s-1).

ρ = particle density (kg m-3).

d_p = particle diameter (m).

g = acceleration due to gravity (m s-2).

C = Cunningham slip-correction factor.$C = 1 + \frac{2\lambda}{d_p}\left(1.257 + 0.4e^{-\frac{0.55 d_p}{\lambda}}\right)$

μ = temperature-dependent viscosity of air (kg m-1 s-1).

λ = the mean free path of air (m).

φ_{hn} = non-dimensional temperature profile constant for neutral conditions.

Z_R = height at which dry deposition velocity is measured (m).

Z_0 = roughness length (m).

Ψ_H = stability correction function for heat (see an example expression in Khan and Perlinger, 2017).

κ = Von Karman constant.

$u_\star$ = friction velocity (m s-1).

E_{Tot} = Total of all deposition process efficiencies: $E_{Tot} = E_B + E_{IM} + E_{IN}$ (see detailed expressions for.E_B, E_{IM}, E_{IN} in Table 2)

E_B = Brownian diffusion efficiency.

E_{IM} = Impaction efficiency.

E_{IN} = Interception F_f = correction factor for convective conditions.$F_f = 1 + 0.24\frac{w_\star^2}{u_\star^2}$

$w_\star$ = convective velocity scale (m s-1).

CAMAERA

- 0D dry deposition intercomparison and evaluation with ground observations over different surfaces-

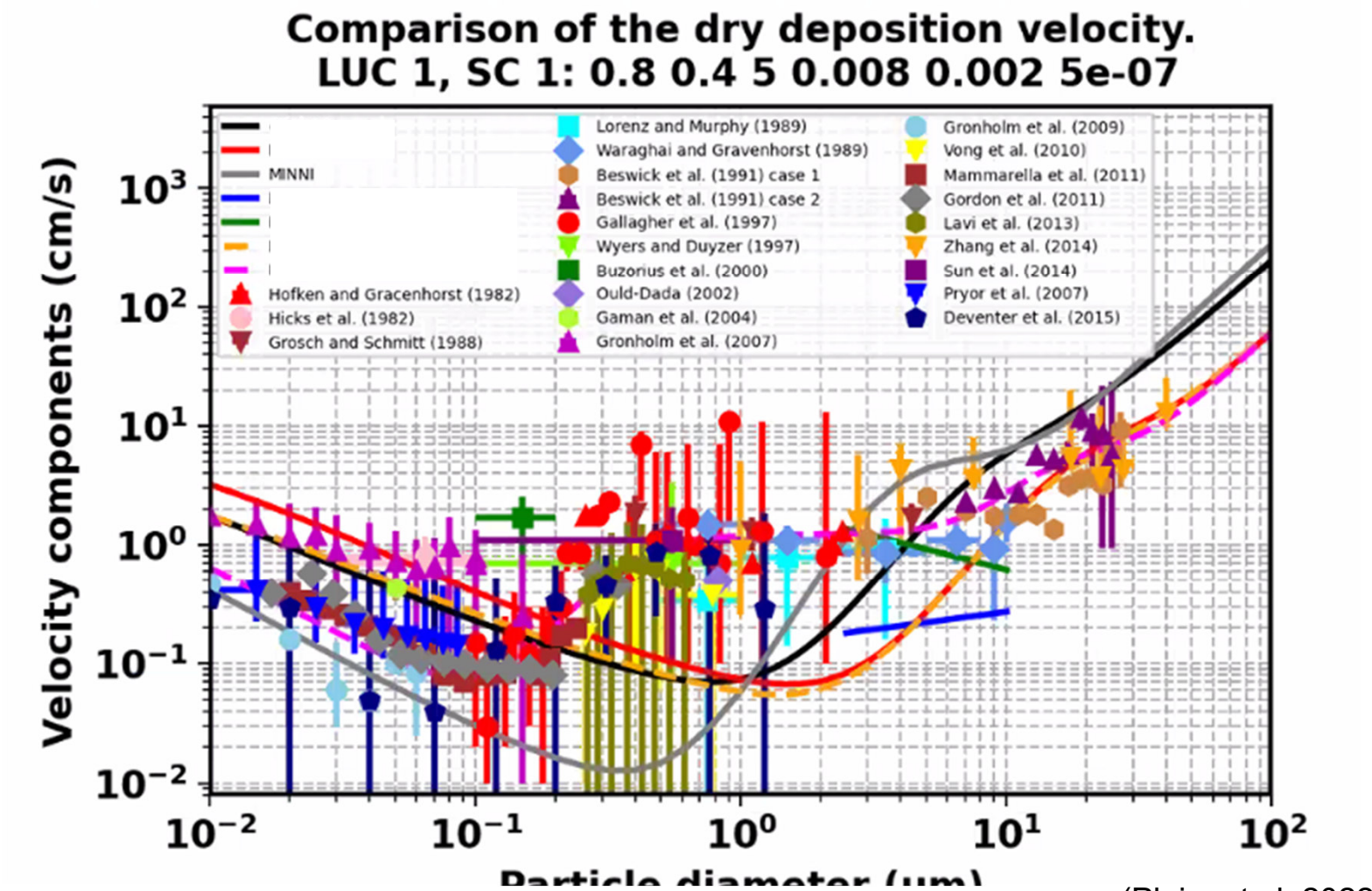

(Pleim et al. 2022)

Z01 in CAMAERA

Table 2
Detailed mechanistic expressions used for particle dry deposition velocity, settling velocity and resistance parameters for monodisperse and sectional approaches.

Scheme	E_B	E_{IM}	E_{IN}	St	E_{IN}	St
			Smooth Surfaces		Vegetative Surfaces	
PR11[a]	$Sc^{-\frac{2}{3}}$	$\frac{St^2}{400+St^2}$	Assume 0	$\frac{V_g u_*^2}{\nu}$	Assume 0	$\frac{V_g u_*^2}{\nu}$
OFF[b]	$Sc^{-\frac{2}{3}}$	$\frac{St^2}{400+St^2}$	Assume 0	$\frac{V_g u_*^2}{\nu}$	Assume 0	$\frac{V_g u_*^2}{\nu}$
VGLAI[c]	$Sc^{-\frac{2}{3}}$	$\frac{St^2}{1+St^2}$	Assume 0	$\frac{V_g u_*}{gA}$	Assume 0	$\frac{V_g u_*}{gA}$
Z01[d]	$Sc^{-\gamma}$	$\left(\frac{St}{\alpha+St}\right)^2$	Assume 0	$\frac{V_g u_*^2}{\nu}$	$\frac{1}{2}\left(\frac{d_p}{A}\right)^2$	$\frac{V_g u_*}{gA}$

γ = empirical parameter dependent on land-use type. Ranges from 0.5 to 0.58.
α = empirical parameter dependent on land-use type. Ranges from 0.8 to 100, but typically 1.0 or 1.2.
ν = kinematic viscosity of air (m2 s-1).
A = characteristic radius of collectors on vegetative surfaces (m).
a, b, c, dSame as Table 1.

Table 3
Parameters for 12 land use categories (LUC) and five seasonal categories (SC)[a]

LUC		1	2	3	4	5	6	7	8	9	10	11	12	13	14	15
Z_0 (m)	SC 1	0.8	2.65	0.85	1.05	1.15	0.1	0.1	0.04	0.03	0.1	0.03	0.01	$f(u)$	$f(u)$	1.0
	SC 2	0.9	2.65	0.85	1.05	1.15	0.1	0.1	0.04	0.03	0.1	0.03	0.01	$f(u)$	$f(u)$	1.0
	SC 3	0.9	2.65	0.80	0.95	1.15	0.05	0.02	0.04	0.03	0.1	0.02	0.01	$f(u)$	$f(u)$	1.0
	SC 4	0.9	2.65	0.55	0.55	1.15	0.02	0.02	0.04	0.03	0.1	0.02	0.01	$f(u)$	$f(u)$	1.0
	SC 5	0.8	2.65	0.60	0.75	1.15	0.05	0.05	0.04	0.03	0.1	0.03	0.01	$f(u)$	$f(u)$	1.0
A (mm)	SC 1	2.0	5.0	2.0	5.0	5.0	2.0	2.0	na	na	10.0	10.0	na	na	na	10.0
	SC 2	2.0	5.0	2.0	5.0	5.0	2.0	2.0	na	na	10.0	10.0	na	na	na	10.0
	SC 3	2.0	5.0	5.0	10.0	5.0	5.0	5.0	na	na	10.0	10.0	na	na	na	10.0
	SC 4	2.0	5.0	5.0	10.0	5.0	5.0	5.0	na	na	10.0	10.0	na	na	na	10.0
	SC 5	2.0	5.0	2.0	5.0	5.0	2.0	2.0	na	na	10.0	10.0	na	na	na	10.0
α		1.0	0.6	1.1	0.8	0.8	1.2	1.2	50.0	50.0	1.3	2.0	50.0	100.0	100.0	1.5
γ		0.56	0.58	0.56	0.56	0.56	0.54	0.54	0.54	0.54	0.54	0.54	0.54	0.50	0.50	0.56

[a]Note: $f(u)$ represents a function of wind speed (u) and na represents not applicable.

Table 2
Land use categories (LUC) and seasonal categories (SC) used in Canadian Aerosol Module

Category	Description
Land use categories (LUC)	
1	Evergreen–needleleaf trees
2	Evergreen broadleaf trees
3	Deciduous needleleaf trees
4	Deciduous broadleaf trees
5	Mixed broadleleaf and needleaf trees
6	Grass
7	Crops, mixed farming
8	Desert
9	Tundra
10	Shrubs and interrupted woodlands
11	Wet land with plants
12	Ice cap and glacier
13	Inland water
14	Ocean
15	Urban
Seasonal categories (SC)	
1	Midsummer with lush vegetation.
2	Autumn with cropland that has not been harvested.
3	Late autumn after frost, no snow.
4	Winter, snow on ground and subfreezing.
5	Transitional spring with partially green short annuals.

CAMAERA

WP9 Consistency between regional and global: intercomparison

WP9 is led by Jacek Kaminski (IOS-PIB) and Samuel Rémy (HYGEOS, project coordinator)

Task 9.1 – Intercomparison regional/global using similar or equivalent emissions (lead HYGEOS, contributor IOS-PIB)

- Merge regional emissions into global so as to run the global system with emissions that are comparable to those of the regional systems
- Comparison of the simulated fields by the regional and global systems, evaluation against observational datasets
- Evaluation of regional and global simulations of the intercomparison using remote sensing products such as AOD and tropospheric columns, depending on the relevance.

CAMEO (CAMs EvOlution)
www.cameo-project.eu

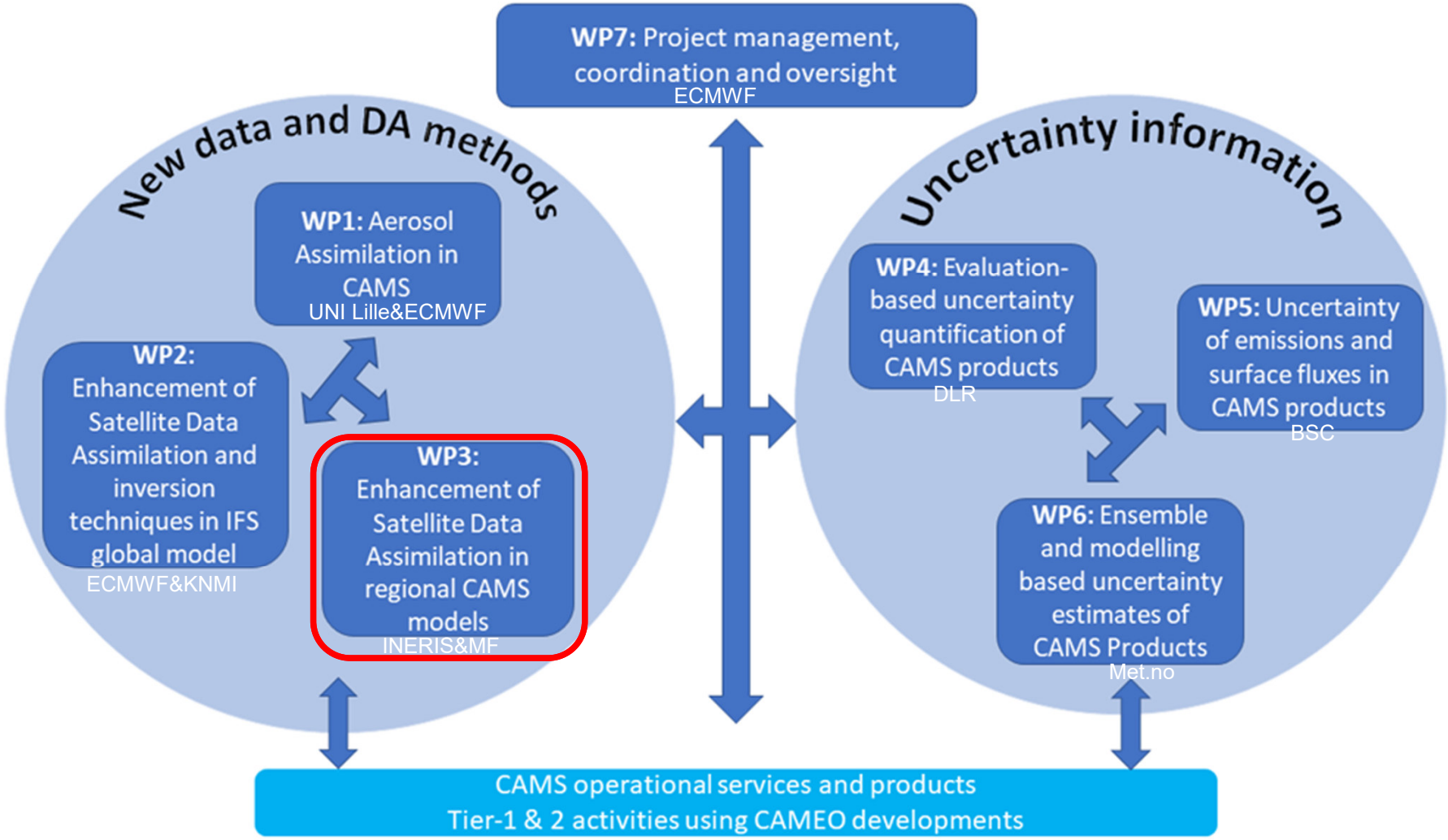

CAMEO – WP3 Enhancement of Satellite Data Assimilation in regional CAMS models

T3.1 Assimilation of Sentinel 5p TROPOMI products (INERIS, FMI, AU, ENEA, FZJ, SMHI, IOS-PIB)

• Task 3.1.1: Assimilation of TROPOMI SO2 in CAMS2_40 Regional Models. All seven teams contributing to Task 1 will assess the added value of assimilating SO2. The assessment will include a sensitivity to the choice of the selected retrieval. The development will be strongly dependent on the individual assimilation techniques in the 7 models participating in Task 1. The coordination will focus on designing consistent numerical plans in the selection of retrieval products and evaluation procedure to demonstrate the added value for the air quality system as a whole.

• Task 3.1.2: Assimilation of TROPOMI CO, O3, HCHO in CAMS2_40 Regional Models. Selected teams will assess the feasibility and added value of assimilating additional gaseous species.

Data Assimilation
-assimilation of measurements at stations-

Data assimilation refers to a large group of methods that update information from numerical computer models with information from observations. Data assimilation is used to update model states, model trajectories over time, model parameters, and combinations thereof.

(Wikipedia)

Atmospheric Environment 306 (2023) 119806

Contents lists available at ScienceDirect

Atmospheric Environment

journal homepage: www.elsevier.com/locate/atmosenv

Data assimilation experiments over Europe with the Chemical Transport Model FARM

Mario Adani [a,*], Francesco Uboldi [b,c,1]

[a] ENEA, Bologna, Italy
[b] Previous affiliation: ARIANET Srl, Milano, Italy
[c] Current affiliation: CIMA Foundation, Savona, Italy

HIGHLIGHTS

- An assimilation scheme based on 3Dvar/O.I. is implemented on CTM FARM model.
- Results are consistent with CAMS ensemble reanalysis.
- Spatial Consistency Test improves model skill scores.
- Advance quality control of assimilated observations improves model estimates.

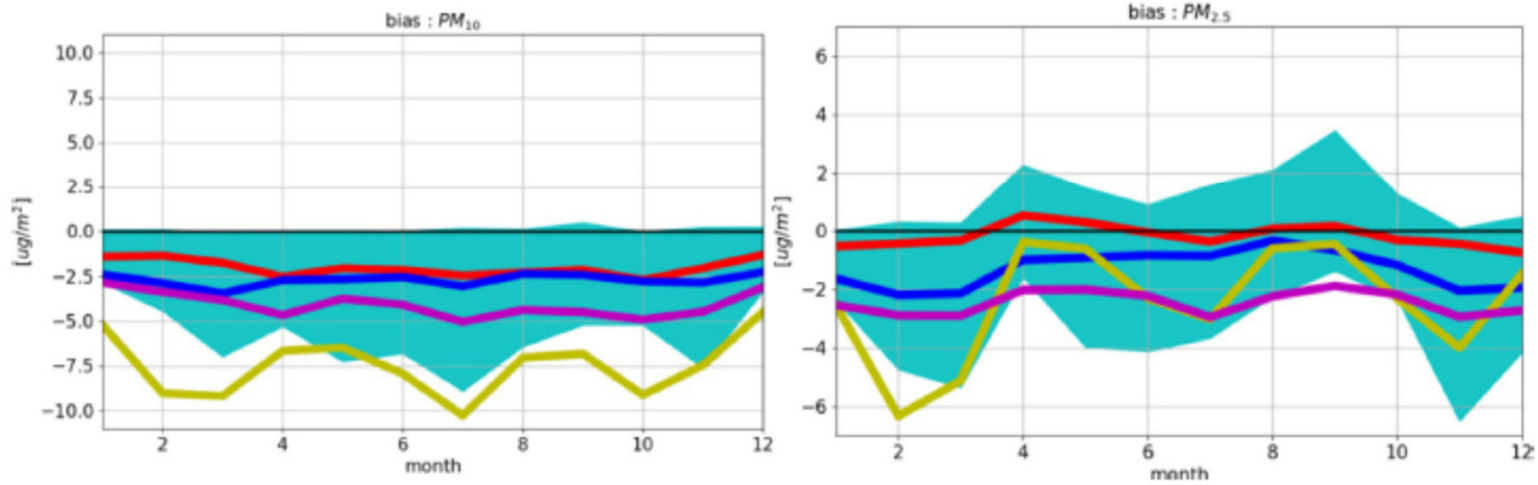

Fig. 4. Median of the monthly bias computed on station for validation. Blue line is the VRA ensemble, red is MINNI with BF and SCT, magenta MINNI with only BF, yellow is the "free run". Shaded area is the spread of CAMS members.

Gen

Data Assimilation
-measurements at stations and satellite data-

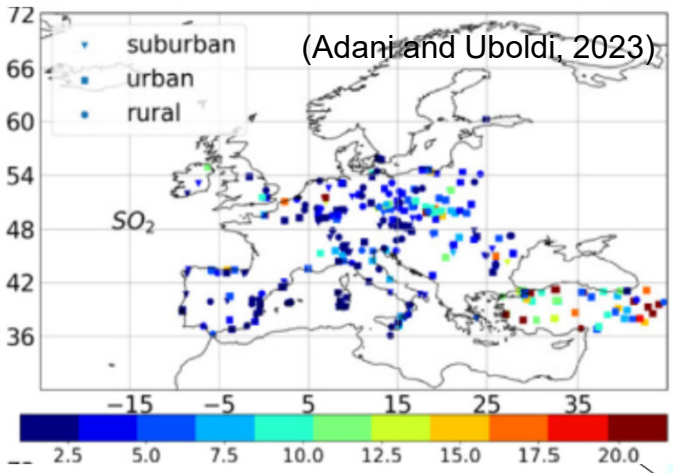

(Adani and Uboldi, 2023)

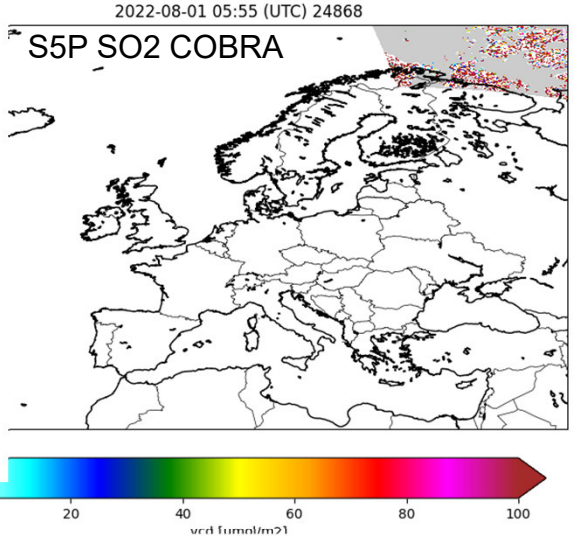

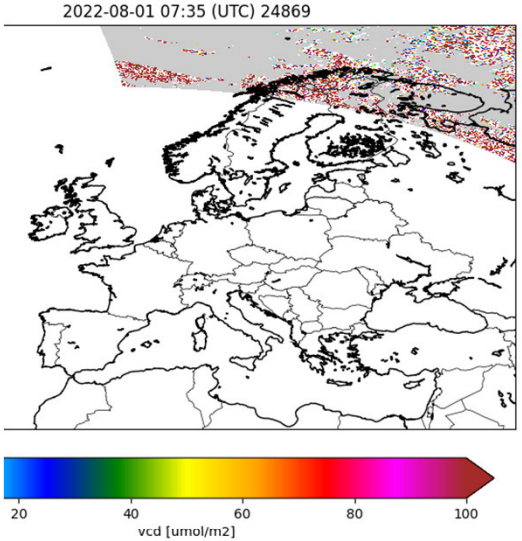

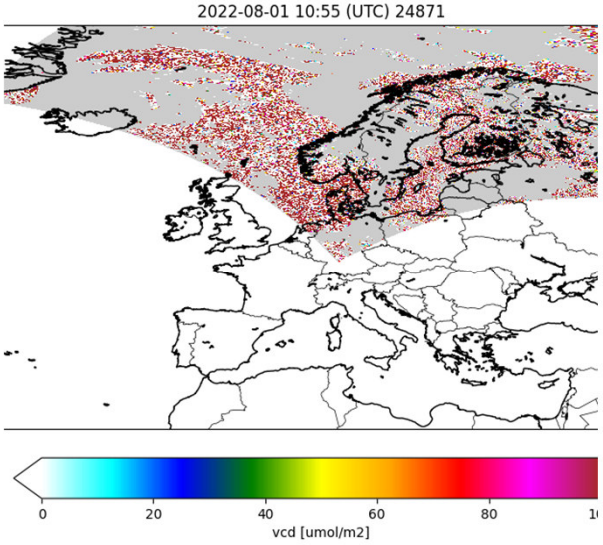

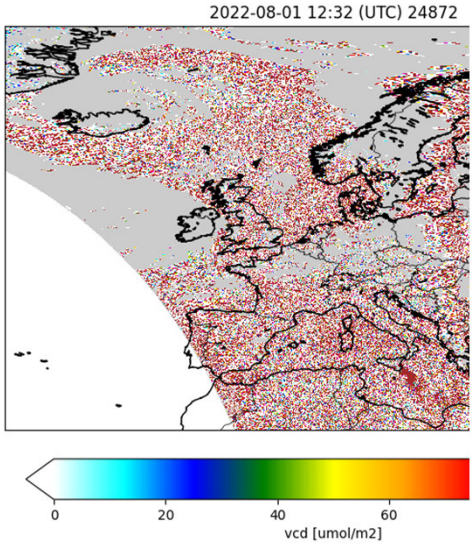

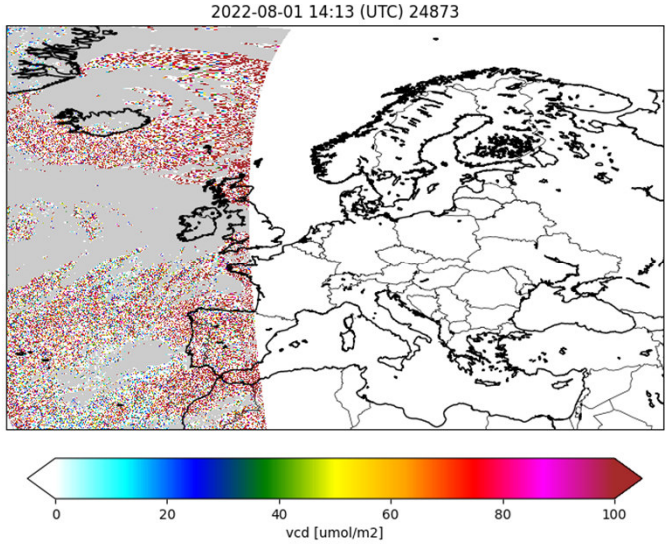

CSO - CAMS Satellite Operator

Tools for assimilation of satellite data in regional air quality model.

Aarjo Segers (https://ci.tno.nl/gitlab/cams/cso)

Observation operator SO2-COBRA (T3.1.1 CAMEO)

A model simulated column is :

$$y_s\ (x_m) = \sum_l A_l\ Hx_{m,l}$$

- x_m is the local model apriori profile
- ***A*** is the averaging kernel defined on the *a priori* layers
- ***H*** is the horizontal and vertical mapping operator from model grid to layers to *a priori* layers

- Possible benefit of using Air Mass Factor (AMF) as reported in the PUM and Duros et al 2023 (https://doi.org/10.5194/gmd-16-509-2023)

- AMF : ratio between optical thickness of vertical and slant vertical column. By default, AMF are provided with TM5 apriori profile.

Alternative AMF is defined by:

$$M_m^*(x_m) = M(x_a)\sum_l A_l\ Hx_{m,l} / \sum_l Hx_{m,l}$$

- x_a is the apriori TM5 profile
- x_m is the local model apriori profile
- $M(x_a)$ is the TM5 airmass factor
- ***A*** is the averaging kernel defined on the *a priori* layers
- ***H*** is the horizontal and vertical mapping operator from model grid to layers to *a priori* layers

Courtesy of Gaël Descombes (INERIS)

Data Assimilation:

Optimal Interpolation (OI) and Ensemble Adjustment Kalman Filter (EnAKF)

OI: the background error covariance matrix is stationary

- It is a static, variance-minimizing method that updates the state estimate using a weighted average of observations and model forecasts.
- The weights are determined based on a predefined covariance matrix, which does not evolve dynamically.
- OI assumes stationary error statistics, meaning it does not adapt to time-varying uncertainties in the system.

Computationally efficient since it uses a precomputed covariance matrix.

Often used in operational weather forecasting where computational efficiency is key.

EnAKF: the background error covariance evolves with the model dynamics

- It is an ensemble-based, sequential assimilation method that updates model states using a dynamically evolving estimate of error covariances.
- Unlike OI, it does not require an explicit model for error covariances; instead, it estimates them from the ensemble of model states.
- EAKF accounts for nonlinear and time-dependent error growth, making it more suitable for highly dynamic systems.

More computationally expensive because it requires running and updating an ensemble of forecasts.

Widely used in modern atmospheric and ocean data assimilation systems (e.g., for climate reanalysis and numerical weather prediction) due to its ability to handle complex error structures.

MINNI simulation setup over Europe: August 2023

resolution	0.15 x 0.1 lat/lon
number grid points	468x421
number of vertical levels	17
top of domain	11790m
meteorological driver	12 UTC IFS, 1 hrly
boundary conditions	CAMS global
Emission inventory	EmissionInventories6.1.1_year2022(operational end of 2024)

OI setup

The most basic mathematical formulation of **Optimal Interpolation (OI)** for **satellite data assimilation** is given by the **analysis equation**:

$$x^a = x^b + K(y - Hx^b)$$

where:

- x^a = **analysis state** (updated estimate of the atmosphere after assimilatio
- x^b = **background state** (forecast or prior estimate).
- y = **observation** (e.g., satellite temperature retrieval).
- H = **observation operator**, which converts the model state to observatio
- K = **Kalman gain matrix**, which determines how much weight is given to observations versus the background.
- $y - Hx^b$ = **observation innovation**, which represents the difference between the observed and predicted values.

Kalman Gain in OI

The **Kalman gain matrix** in OI is computed as:

$$K = BH^T(HBH^T + R)^{-1}$$

where:

- B = **background error covariance matrix** (describes uncertainty in the background state).
- R = **observation error covariance matrix** (describes uncertainty in satellite observations).
- H^T = **transpose of the observation operator**, which transforms observation space back into model space.

Optimal Interpolation
Background Error Covariance Matrix (B) computed with NMC (Parrish and Derber, 1992) for 48h-0h forecast (D0 and D-2) using log concentration
B annual (average of monthly B), static
Negative values are not considered
Satellite data assimilated only if they are two times higher than their St.Dev
Observational Error Covariance Matrix (R) extracted from satellite data
B and R are diagonal: variance and correlation scales are handled separately

SO2 COBRA dataset assimilation with OI

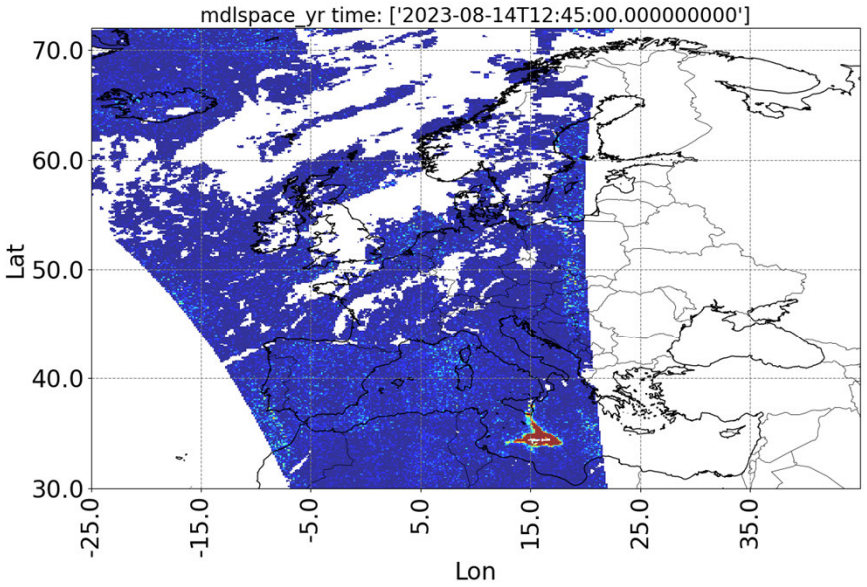

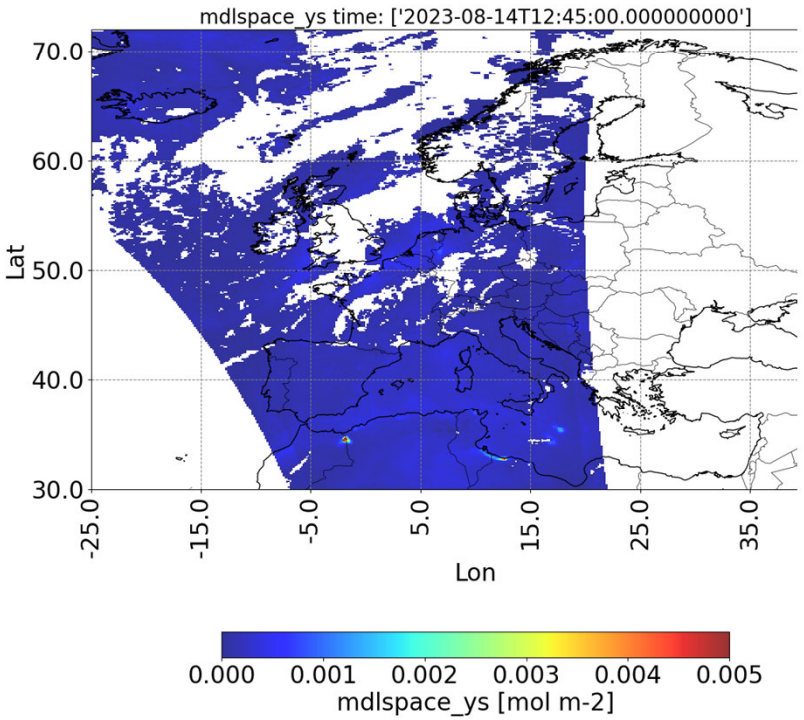

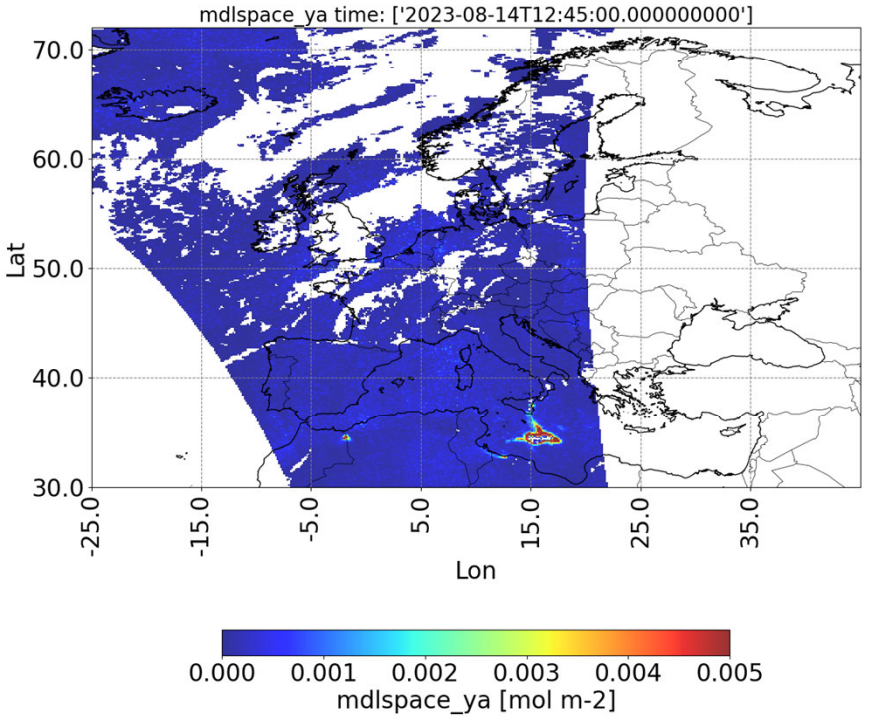

SO2 COBRA dataset assimilation with OI

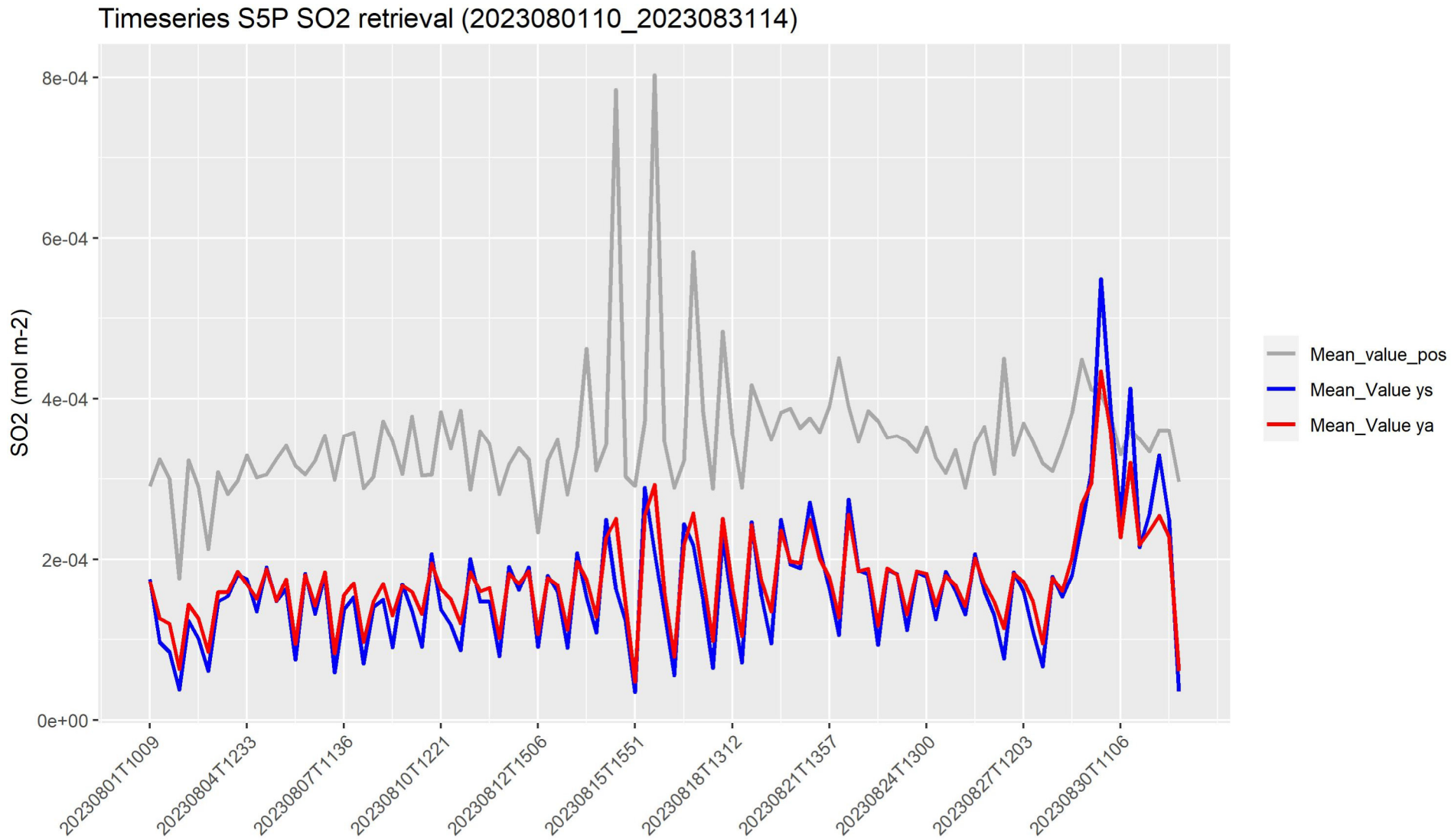

NO_2 dataset assimilation with OI

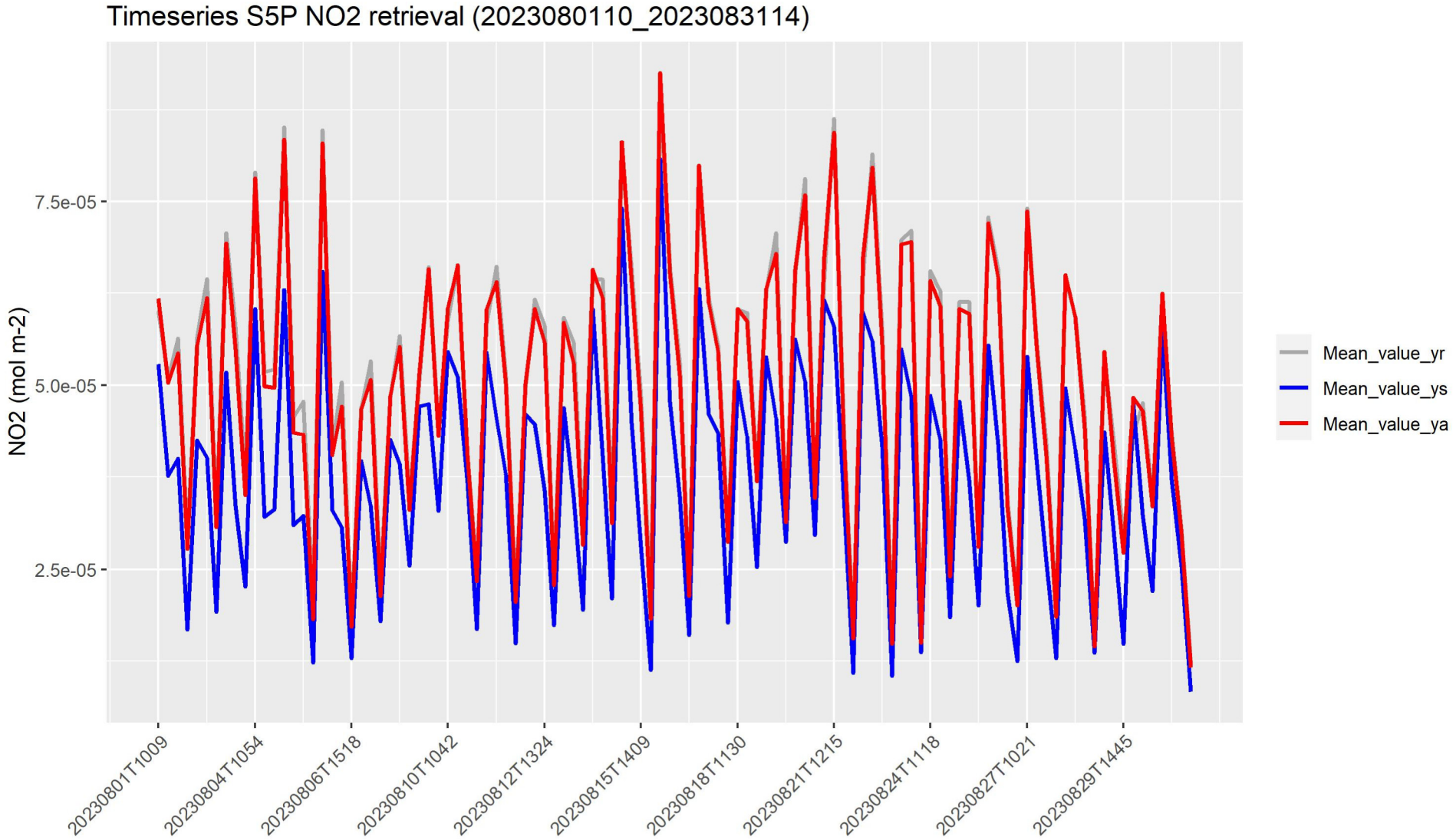

EnAKF-DART implementation in MINNI

Ensemble Adjustment Kalman Filter (EnAKF)

Analysis equation

$$x_i^a = x_i^f + K_i\left(y^o - H_i x_i^f\right)$$

Kalman Gain

$$K_i = P_i^f H_i^T \left(H_i P_i^f H^T + R_i\right)^{-1}$$

EnKFI: Replacement large covariance matrices with ensemble statistics

$$\bar{x_i} = \frac{1}{m}\sum_{k=1}^{m} x_i^{f(k)} \qquad \delta x^f = x_i^{f(k)} - \bar{x_i}, \qquad \delta x^f = \left[\delta x^{f(1)} \ldots . \delta x^{f(m)}\right] \in R^{NXm}$$

The forecast error covariance matrix P^f can be approximated as

$$P^f \approx \frac{1}{m-1}\delta x^f \delta x^{fT}$$

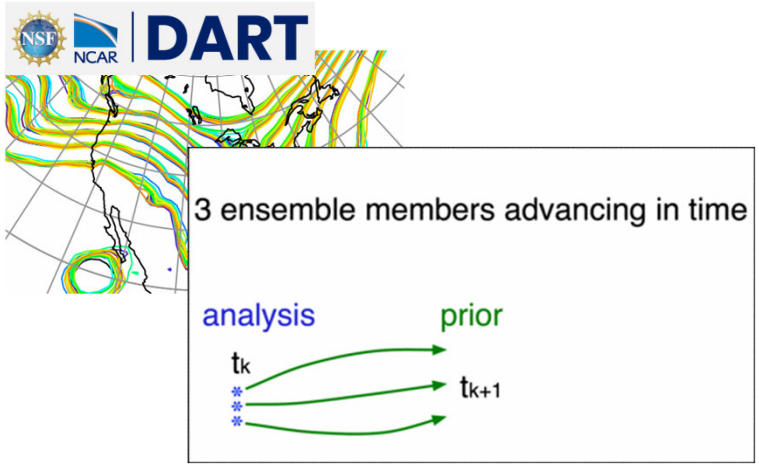

Ensemble Adjustment Kalman Filter
EnAKF provides a deterministic update of the forecast ensemble (ensemble square root filters)
True state / background covariance matrix: $m \rightarrow \infty$
m usual range : 15 -100
m low: - sampling noise, off-diagonal terms in P_i^f - Filter divergence due to insufficient variance
Sampling noise mitigation: **covariance localization function** (smooth-off) to avoid spurious long-range correlations / lost of far flow dependency structures
Filter divergence: **inflation** techniques
Quantile conserving Ensemble Filtering framework (**QCEFF**)

[1] Welcome to the Data Assimilation Research Testbed — DART 11.10.6 documentation

EnAKF-DART: Perturbations

- Adds noise to emissions while maintaining user-defined vertical/horizontal correlation.
- Prevent ensemble collapse (zero spread) by fine-tuning parameters (horiz/vert/spread).
- Well-suited for correcting concentration fields influenced by emissions.
- No inclusion of volcanic emissions
- Emission ensemble mean centered on reference base case

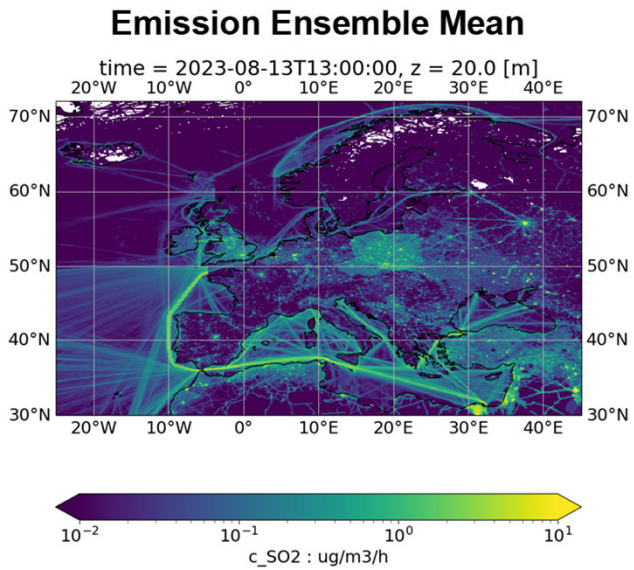

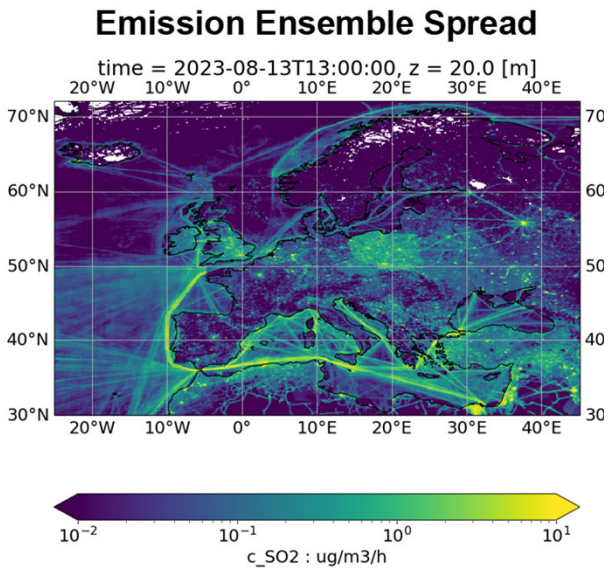

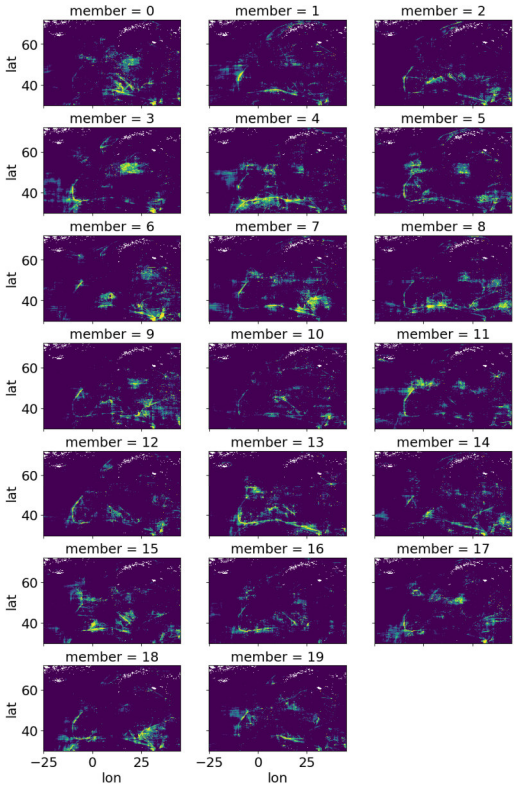

Left: Mean sulfur dioxide (SO_2) emissions from the ensemble. Right: Ensemble spread (uncertainty) in SO_2 emissions. Datetime: 2023-08-13 13:00

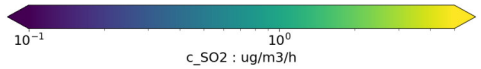

FARM-DART
Implementation and performances

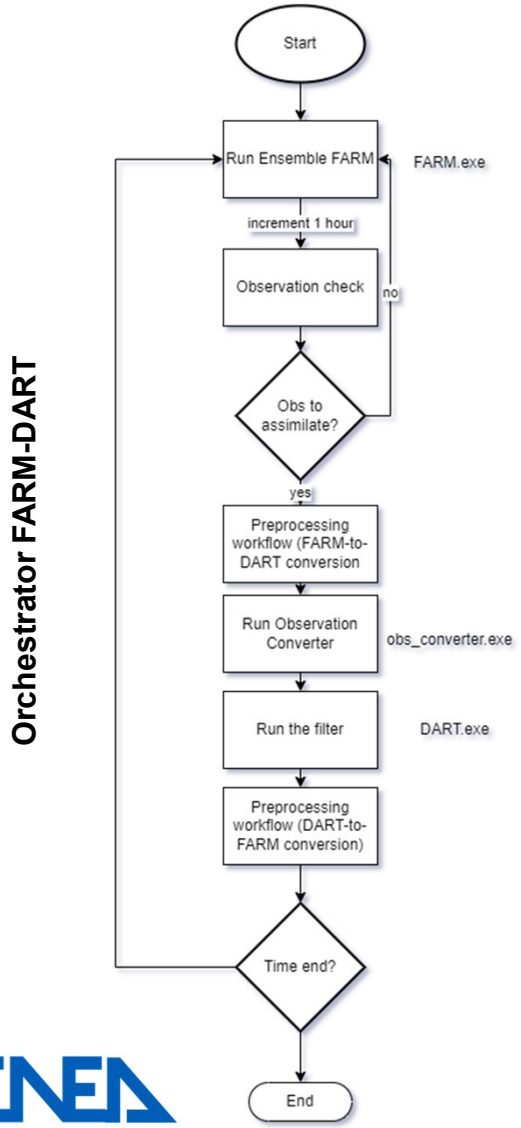

CRESCO6 HPC, Intel Xeon Platinum 8160 CPUs with 48 cores per node (24 cores per socket, 2 sockets).

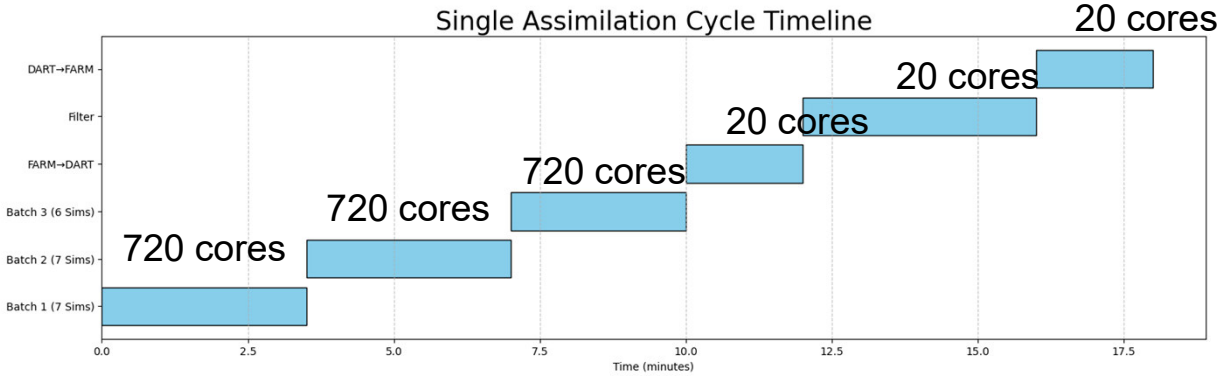

10 minutes per cycle = 6 days total runtime

EnAKF-DART results – August 2023 (obs space)

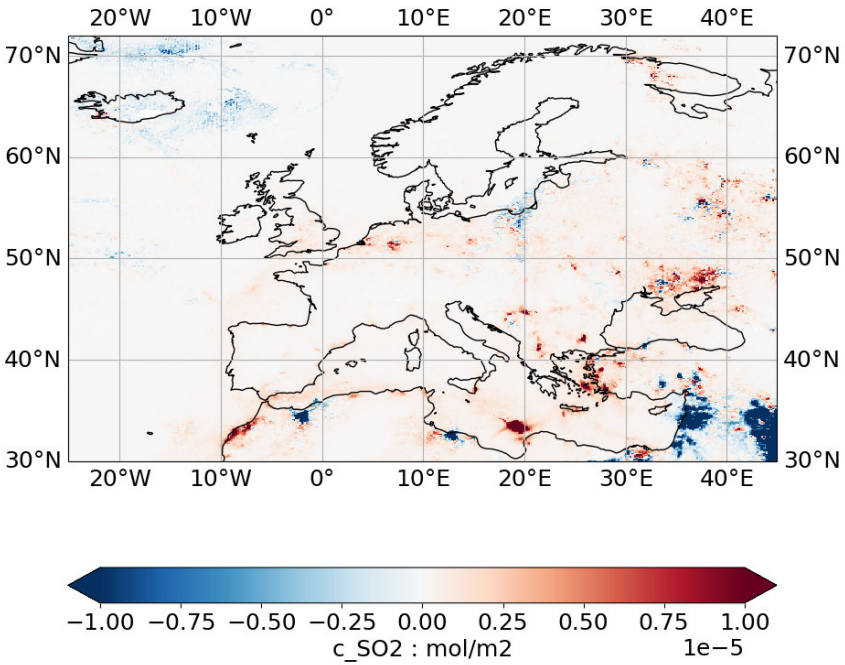

Averaged difference between Posterior and Prior ensemble means

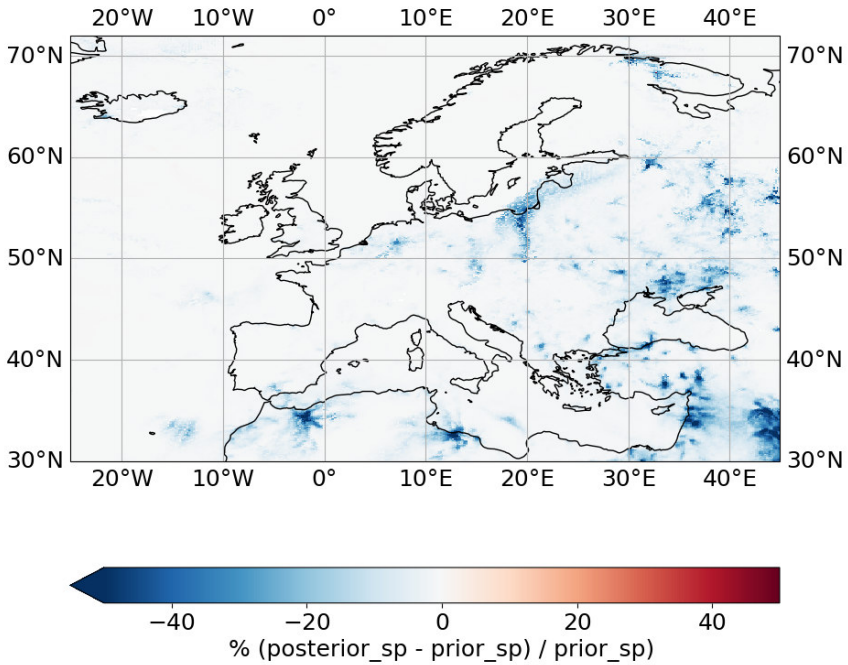

Relative difference between posterior and prior ensemble spread over Europe

EnAKF-DART results – August 2023 (model space)

Averaged difference between Posterior and Prior ensemble means

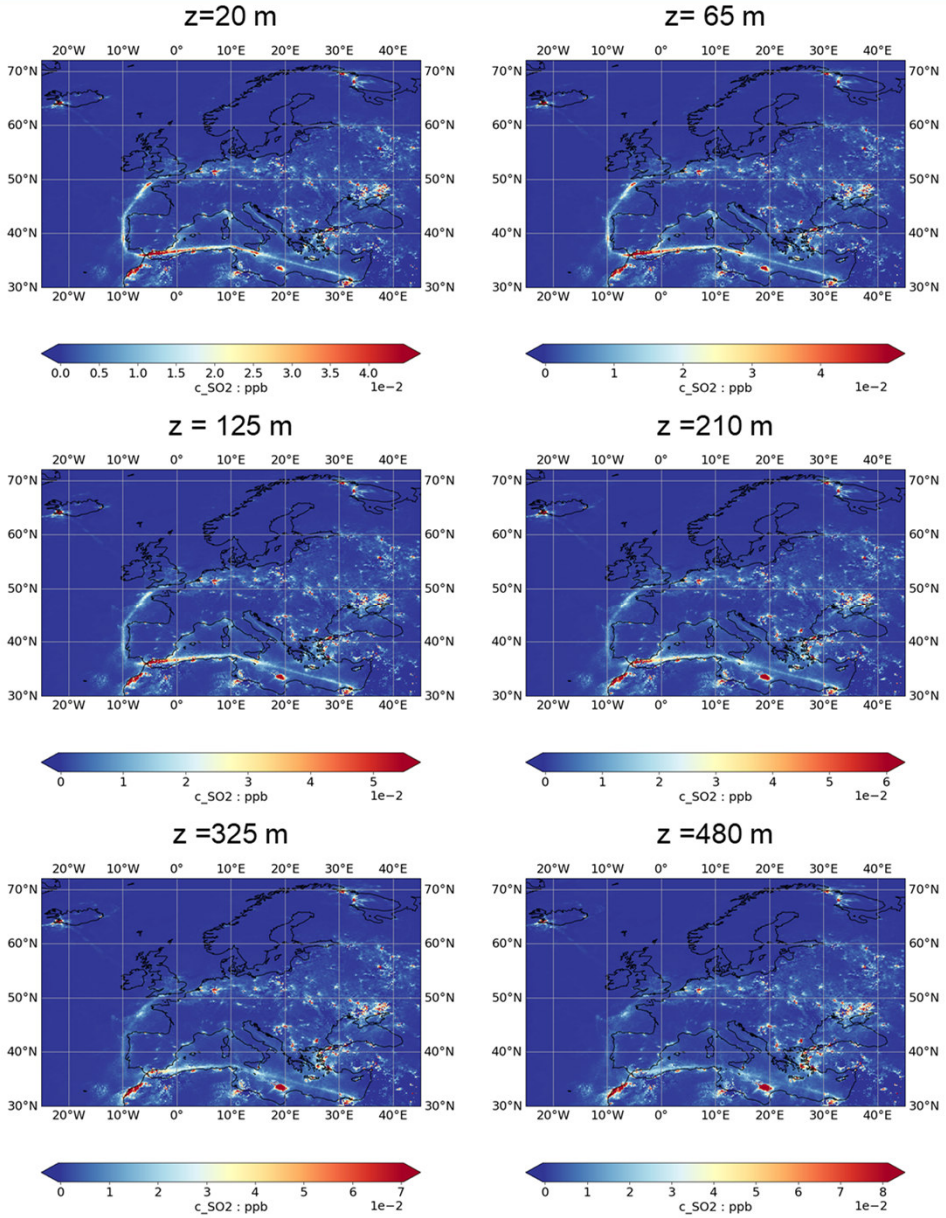

Small corrections possibly due to:

- Insufficient spread from perturbations
- Lack of volcanic emissions

Sensitivity analysis: emission perturbations

Changing perturbation -> redefinition of background error covariance matrix

Perturbations centered on basecase

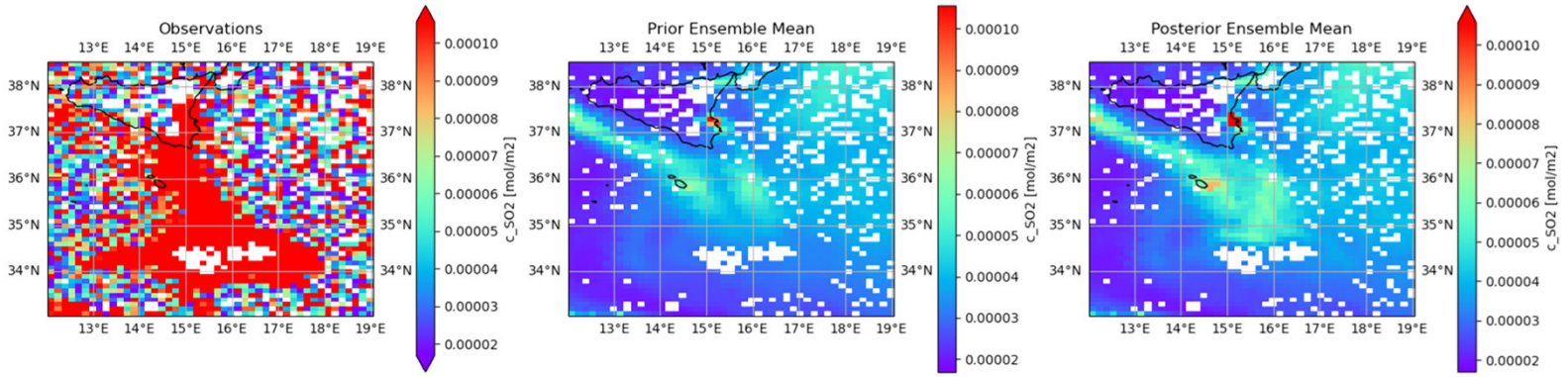

Perturbations not centered on basecase

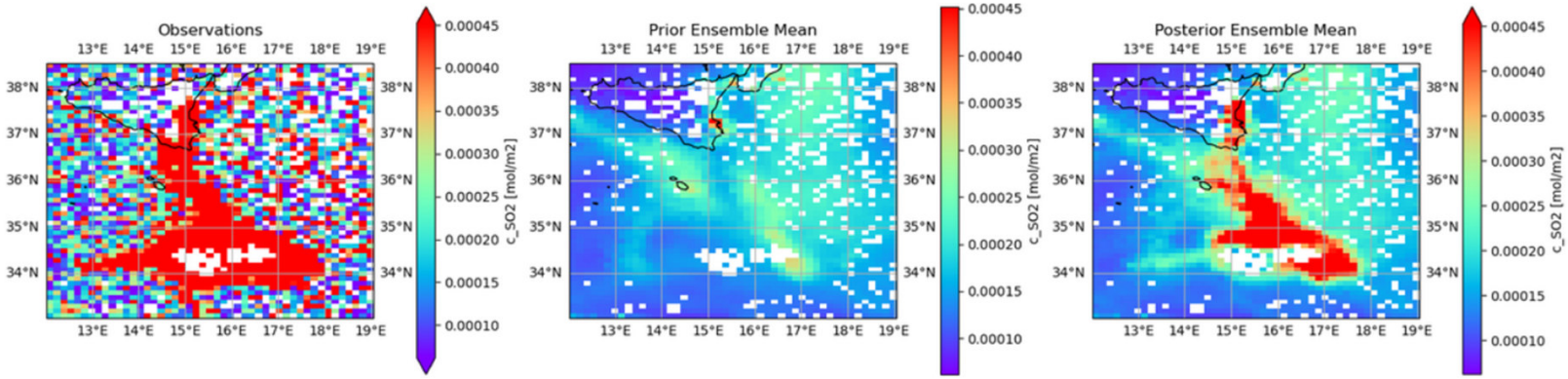

Results: emission perturbations

Corrections to ground level

Observation space

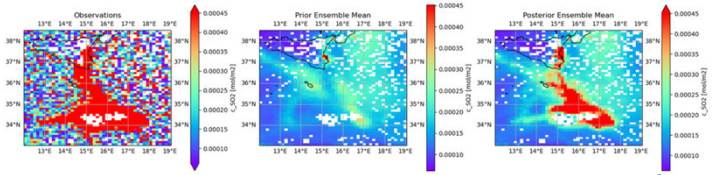

Model Space (level 20 m)

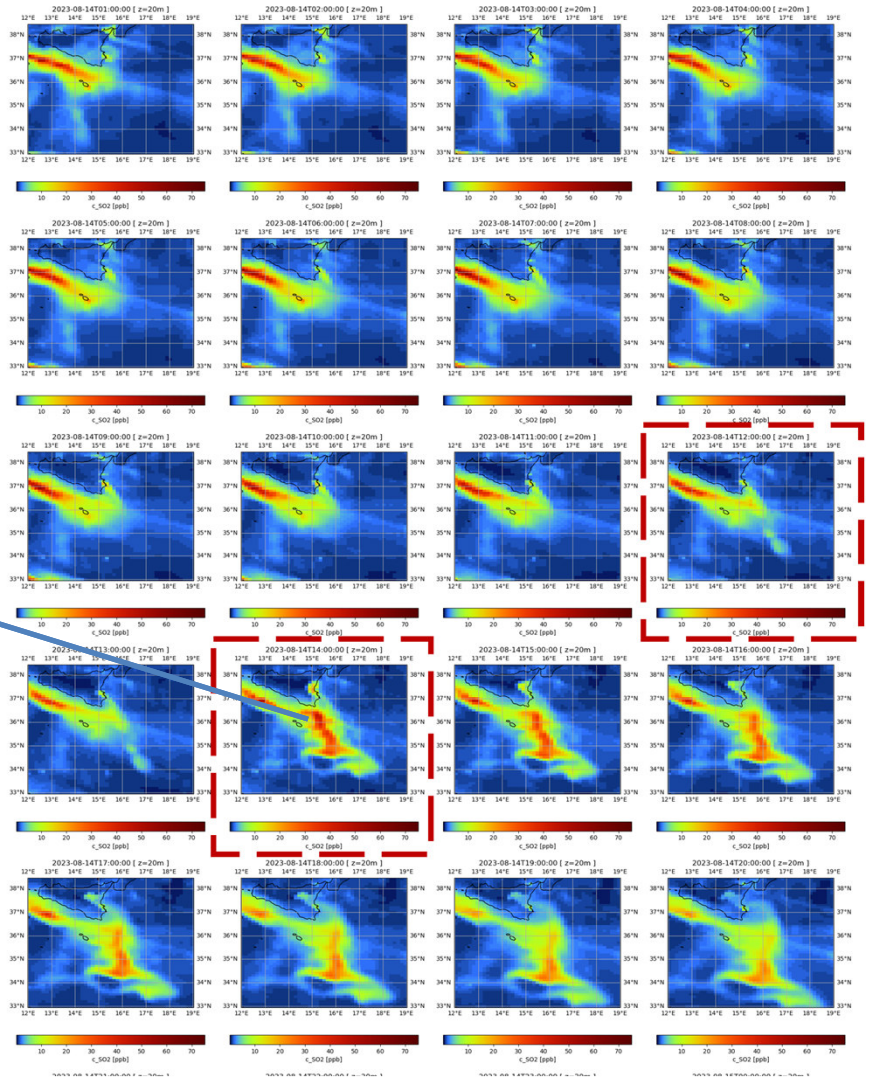

Summary and future plans

-SO2 satellite data assimilation with OI makes “visible” Etna plume more than EnAKF-DART with current setup

-HCHO, CO and O3 satellite data will be assimilated with OI and at least one pollutant with EnAKF-DART

-study the sensitivity of OI results to background error covariance matrix specification

-study the sensitivity of SO2 results with EnAKF-DART to perturbation parameters and prior inflation

-study if EnAKF-DART performances improves when SO2 Etna emissions will be included

EGU 2025

EGU General Assembly 2025

EDI
Atmospheric Composition and Numerical Weather Forecasting
Co-sponsored by WMO and CAMS
Convener: Johannes Flemming
Co-conveners: Alexander Baklanov, Georg Grell, Sara Basart
▸ Orals | Tue, 29 Apr, 10:45–12:25 (CEST) Room M1
▸ Posters on site | Attendance Tue, 29 Apr, 14:00–15:45 (CEST) | Display Tue, 29 Apr, 14:00–18:00 Hall X5
▸ Posters virtual | Attendance Wed, 30 Apr, 14:00–15:45 (CEST) | Display Wed, 30 Apr, 14:00–18:00 vPoster spot 5

Session description

Orals: Tue, 29 Apr | Room M1

> The oral presentations are given in a hybrid format supported by a Zoom meeting featuring on-site and virtual presentations. The button to access the Zoom meeting appears just before the time block starts.

Chairpersons: Johannes Flemming, Sara Basart, Alexander Baklanov

12:15–12:25 | EGU25-16042 | ECS | On-site presentation
Assessing the impacts of assimilating SO2 TROPOMI retrievals with MINNI and DART at the European scale: a case study of the Mount Etna eruption ▸
Alessandro D'Ausilio, Giorgia De Moliner, Camillo Silibello, Andrea Bolignano, Gino Briganti, Felicita Russo, and **Mihaela Mircea**

ENEA

EGU 2025

EDI
Satellite observations of tropospheric composition and pollution, analyses with models and applications
Convener: Andreas Richter
Co-conveners: Shima Bahramvash Shams, Cathy Clerbaux, Pieternel Levelt
▸ Orals | Mon, 28 Apr, 14:00–18:00 (CEST) Room 0.11/12
▸ Posters on site | Attendance Mon, 28 Apr, 10:45–12:30 (CEST) | Display Mon, 28 Apr, 08:30–12:30 Hall X5
▸ Posters virtual | Attendance Wed, 30 Apr, 14:00–15:45 (CEST) | Display Wed, 30 Apr, 14:00–18:00 vPoster spot 5

Session description

Orals: Mon, 28 Apr | Room 0.11/12

The oral presentations are given in a hybrid format supported by a Zoom meeting featuring on-site and virtual presentations. The button to access the Zoom meeting appears just before the time block starts.

Chairpersons: Andreas Richter, Shima Bahramvash Shams

Posters on site: Mon, 28 Apr, 10:45–12:30 | Hall X5

The posters scheduled for on-site presentation are only visible in the poster hall in Vienna. If authors uploaded their presentation files, these files are linked from the abstracts below.

Display time: Mon, 28 Apr, 08:30–12:30

X5.19 | EGU25-16722
Assimilation of SO2, CO, HCHO and O3 satellite data with Optimal Interpolation implemented in Atmospheric Modelling System MINNI ▸
Andrea Bolignano, Mario Adani, Gino Briganti, Felicita Russo, and **Mihaela Mircea**